Nonpolar Interactions of Thrombin and Its Inhibitors at the Fibrinogen Recognition Exosite: Thermodynamic Analysis†

Yudu Cheng, Jacek J. Slon-Usakiewicz, Jing Wang, Enrico O. Purisima, and Yasuo Konishi*

National Research Council of Canada, Biotechnology Research Institute, 6100 Royalmount Avenue, Montreal, Quebec, Canada H4P 2R2

Received May 1, 1996⊗

ABSTRACT: Nonpolar interactions play a major role in the association of the fibrinogen recognition exosite of thrombin with the C-terminal fragment (55−65), Asp-Phe-Glu-Glu-Ile-Pro-Glu-Glu-Tyr-Leu-Gln, of hirudin, which is a naturally occurring thrombin inhibitor. The thermodynamic details (free energy, enthalpy, entropy, and heat capacity) of the molecular recognition are studied by using five analogs of a synthetic bivalent thrombin inhibitor (P552), *tert*-butylbenzensulfonyl-Arg-(D-pipecolic acid)-(12-amino-dodecanoic acid)-(γ-aminobutyric acid)-hirudin$^{55-65}$. The residue of Phe^{H56}, Ile^{H59}, Pro^{H60}, Tyr^{H63}, or Leu^{H64} in hirudin$^{55-65}$ segment is substituted by Gly in each analog in order to elucidate the contributions of these nonpolar side chains. The results show that the interactions of these nonpolar side chains with thrombin are enthalpy-driven, except for the contribution of the Phe^{H56} side chain which is entropy-driven. Interestingly, molecular modeling predicts a large conformational change due to the Gly substitution of Phe^{H56}. In analyzing the correlation among the thermodynamic and structural properties of the nonpolar interaction, a good correlation is observed between the binding free energy and the hydrophobicity of the molecular surface; i.e., tighter binding is observed as more nonpolar atoms are buried and more polar atoms are exposed upon molecular association.

Thrombin is a key enzyme regulating thrombosis in cardiovascular disease (Gould & Shafer, 1993; Lefkovits & Topol, 1994). Many thrombin inhibitors have been developed to prevent reocclusion after treatment of thrombus with tissue plasminogen activator or urokinase. Some of them are based on the sequence of hirudin produced in the salivary glands of the European medicinal leech *Hirudo medicinalis*. Hirudin, a 65 amino acid protein, is the most potent and specific thrombin inhibitor with a K_i value of 2.2×10^{-14} M (Stone & Hofsteenge, 1986). The tight binding arises from the simultaneous binding of the N-terminal hirudin$^{1-48}$ segment and the C-terminal hirudin$^{55-65}$ segment to the active site and the fibrinogen recognition exosite (FRE)[1] of thrombin, respectively (Markwardt, 1989; Rydel et al., 1990, 1991). The N-terminal 48 residues of hirudin have 3 disulfide bonds with a rigid structure. Indeed, the crystal structure of the hirudin$^{1-48}$ segment in complex with thrombin (Rydel et al., 1990, 1991; Grütter et al., 1990) is very similar to its solution structure in the absence of thrombin (Clore et al., 1987; Folkers et al., 1989; Haruyama & Wüthrich, 1989). On the other hand, the C-terminal 11 residues of hirudin have a flexible conformation in solution and fold to a well-defined structure upon binding to the FRE. The FRE and hirudin$^{55-65}$ show complementary sequences such that basic and hydrophobic residues dominate the FRE whereas hirudin$^{55-65}$ is enriched by acidic and hydrophobic residues as -Asp^{H55}-Phe-Glu-Glu-Ile-Pro^{H60}-Glu-Glu-Tyr-Leu-Gln^{H65}-OH.[2] The electrostatic interaction contributes to the association rate constant (Stone & Hofsteenge, 1986; Stone et al., 1989; Karshikov et al., 1992); however, the hydrophobic interactions predominantly stabilize the complex (Yue et al., 1992; Tsuda et al., 1995). Betz et al. (1991) studied the effects of Phe^{H56}, Pro^{H60}, and Tyr^{H63} by mutating them to various amino acids and suggested (1) a strong preference of aromatic amino acids at the 56th residue of hirudin, (2) a ∼10-fold increase of the K_i value by mutating Pro^{H60} to Ala or Gly, and (3) a rather low sequence specificity of the 63rd residue. Interestingly, in all mutants, the decrease of the affinity is due to the decrease of the association rate constant.

The association constant of an inhibitor (K_a) is the inverse of the dissociation constant (K_d), which is approximated by the inhibition constant (K_i) measured. Thus, the binding free energy (ΔG), enthalpy (ΔH), entropy (ΔS), and heat capacity (ΔC_p) may be expressed as

$$\begin{aligned}\Delta G^\circ(T) &= [\Delta H^\circ(T^\circ) - T\Delta S^\circ(T^\circ)] + \Delta C_p[(T - T^\circ) - T\ln(T/T^\circ)] \\ &= -RT\ln K_a \\ &= RT\ln K_d \\ &\cong RT\ln K_i \end{aligned} \quad (1)$$

where 1.0 mol/L is the standard state for all chemical species

† NRCC Publication No. 39903.

* Author to whom correspondence should be addressed.

⊗ Abstract published in *Advance ACS Abstracts,* September 15, 1996.

[1] Abbreviations: γAbu, γ-aminobutyric acid; Ac, acetyl; μAdod, 12-aminododecanoic acid; AMC, 7-amino-4-methylcoumarin; ζAhp, 7-aminoheptanoic acid; Bbs, 4-*tert*-butylbenzenesulfonyl; Fmoc, 9-fluorenylmethoxycarbonyl; FRE, fibrinogen recognition exosite; HPLC, high-performance liquid chromatography; K_m, Michaelis constant; Pip, pipecolic acid; PPACK, D-Phe-Pro-Arg chloromethyl ketone; TFA, trifluoroacetic acid; Tos, tosyl; Tris, 2-amino-2-(hydroxymethyl)-1,3-propanediol; λ_{ex}, excitation wavelength; λ_{em}, emission wavelength; v, initial velocity; V_{max}, maximal velocity.

S0006-2960(96)01039-2 CCC: $12.00 Published 1996 by the American Chemical Society

and $T°$ is the reference temperature (25 °C in this paper). The standard-state free energy at arbitrary temperature T is obtained from the standard-state enthalpy and entropy at the reference temperature, $T°$, plus a correction term that reflects the temperature dependence of ΔH and ΔS. In general, ΔH is a binding energy and has contributions from the van der Waals interactions, hydrogen bonding interaction, dehydration, and other effects (e.g., deprotonation, ion-bridge, etc.). ΔS is the entropy change arising, for example, from rotational and translational degrees of freedom that are restricted upon complex formation. Reorganization of solvent structure also contributes to ΔS. ΔC_p measures the temperature dependence of ΔH and ΔS and is often presumed to be proportional to the solvent-accessible surface areas of polar and nonpolar atoms (Baldwin, 1986; Spolar et al., 1989, 1992; Murphy et al., 1990; Murphy & Freire, 1992; Makhatadze & Privalov, 1993). ΔC_p is assumed to be temperature-independent in eq 1.

Thrombin interactions have been analyzed thermodynamically using natural and synthetic substrates (Hopfner & Di Cera, 1992) and inhibitors (Hopfner et al., 1993). A Krug−Hunter−Greiger plot of ΔH and ΔG shows that tighter substrate binding is achieved by the decrease of enthalpy (enthalpy-driven), whereas tighter bivalent inhibitor binding is achieved by the increase of entropy (entropy-driven). For example, the complexation of thrombin and recombinant hirudin actually increases the entropy. The thrombin interactions with the substrates and inhibitors include hydrophobic, ionic, and hydrogen-bonded interactions as well as solvent exclusion, and these interactions may have different thermodynamic contributions to the binding. Since the hydrophobic interaction plays a critical role in thrombin interactions (Yue et al., 1992; Tsuda et al., 1995), this study aims to analyze the thermodynamic contributions of five nonpolar residues (Phe^{H56}, Ile^{H59}, Pro^{H60}, Tyr^{H63}, and Leu^{H64}) of hirudin in the association to the FRE. Consequently, five analogs of a synthetic bivalent inhibitor, P552, are prepared by substituting Phe^{H56}, Ile^{H59}, Pro^{H60}, Tyr^{H63}, or Leu^{H64} by Gly. The temperature dependence of the inhibition constants of these inhibitors provides the thermodynamic properties (free energy, enthalpy, entropy, and heat capacity) of these nonpolar side chains, which are then correlated with the structural features studied by molecular modeling.

EXPERIMENTAL PROCEDURES

Materials. Human α-thrombin (3000 NIH units/mg, containing bovine serum albumin as a stabilizer), the fluorogenic substrate (Tos-Gly-Pro-Arg-AMC·HCl), Trizma pre-set crystal (pH 7.80 at 25 °C), and poly(ethylene glycol) 8000 were purchased from Sigma. Sodium phosphate monobasic and NaCl were obtained from Anachemia and Fisher Scientific, respectively. Bbs and dimethyl sulfoxide used to dissolve the substrate were obtained from Aldrich. Fmoc-D-Pip and Fmoc-γAbu were purchased from BaChem Bioscience Ind. Fmoc-μAdod was prepared as described by Chaturvedi et al. (1984). Other Fmoc derivatives of amino acids were purchased from Advanced ChemTech and Novabiochem. *N*-α-Fmoc-*N*-γ-trityl-L-Gln-Wang resin was purchased from Applied Biosystem Inc. The solvents used in peptide synthesis were obtained from Anachemia Chemical Inc. and Applied Biosystems Inc.

Peptide Synthesis. The thrombin inhibitors are synthesized on a 396 Multiple Peptide Synthesizer (Advanced ChemTech) by using a conventional Fmoc strategy of solid-phase peptide synthesis. Double couplings are performed throughout the synthesis. After the synthesis, the peptides are cleaved from the resin using Reagent K (TFA, 82.5%; water, 5%; thioanisole, 5%; phenol, 5%; and ethanediol, 2.5%; 25 mL/g of the resin) for ∼4 h at room temperature on the synthesizer. The peptides are, then, precipitated with diethyl ether and washed 3 times with diethyl ether to remove the protecting groups and the scavengers. The peptides are dissolved in 50% acetic acid and lyophilized. The peptides are then purified by preparative HPLC (Vydac C_4 column, 4.6 × 25 cm) using a linear gradient of 20−50% acetonitrile in 0.1% TFA (0.5%/min gradient, 33 mL/min flow rate). The final products, with ≥98% purity estimated by an analytical HPLC (Vydac C_{18}, 0.46 × 25 cm column) using a linear gradient of 10−70% acetonitrile in 0.1% TFA (1.0%/min gradient, 1.0 mL/min flow rate), are lyophilized. The elution profile is monitored by the absorbance at 215 and 254 nm on the analytical HPLC and at 220 nm on the preparative HPLC. The purified peptides are identified with a Beckman Model 6300 amino acid analyzer and a SCIEX API III mass spectrometer. Amino acid analysis is conducted for peptide content determination. All the peptides used have correct amino acid compositions and molecular mass.

Amidolytic Assay. The inhibition of the amidolytic activity of human α-thrombin is measured using Tos-Gly-Pro-Arg-AMC as a fluorogenic substrate in 50 mM Tris·HCl buffer (pH 7.80 at 25 °C) containing 0.1 M NaCl and 0.1% poly(ethylene glycol) 8000 (Szewczuk et al., 1992) at various temperatures from 10 to 45 °C. The pH of 50 mM Tris·HCl buffer (pH 7.80 at 25 °C) in the presence of 0.1 M NaCl and 0.1% poly(ethylene glycol) 8000 has a temperature variation of −0.027 pH unit/°C (Di Cera et al., 1991). This temperature dependence is ignored in this study because the pH dependence of thrombin activity (K_m and k_{cat}) in this pH range (7.26 at 45 °C to 8.21 at 10 °C) is negligible (Di Cera et al., 1991). Human α-thrombin is stable in this temperature range in the presence of poly(ethylene glycol) (Borgne & Graber, 1994). The final concentrations of the inhibitors, the substrate, and human α-thrombin are 0.3−100-fold of the K_i values in the temperature range of 10−45 °C, 40 μM and 30 pM, respectively. The temperature dependence of K_m and V_{max} is measured at 1−40 μM and 30 pM of the substrate and thrombin, respectively, for 5 min in the absence of inhibitor. Due to the temperature dependence of K_m, 40 μM of the substrate concentration corresponds to 0.8−15-fold of K_m in the temperature range of 10−45 °C. A Hitachi F2000 spectrophotometer and a Perkin Elmer LS50B luminescence spectrometer are used to monitor the enzyme reaction with 383 nm of λ_{ex} and 455 nm of λ_{em}. The temperature of the reaction solutions is controlled using a HAAKE Circulator (HAAKE K15 & DC3, Germany) and monitored using a YSI Series 400 Probe with a digital thermometer (±0.1 °C, VWR Scientific). The stock solutions of the substrate (=7.39 mM) and the inhibitor (=1.00 μM) are mixed in a disposable fluorometer cuvette (SARSTEDT, Germany), and the volume of the mixed solution is adjusted to 2990 μL with 50 mM Tris·HCl buffer

[2] The numbering of the inhibitor residues is based on the hirudin sequence, and "H" is added to the residue number, e.g., Phe^{H56}. The numbering of human α-thrombin residues is based on the chymotrypsin sequence.

(pH 7.80 at 25 °C) containing 0.1 M NaCl and 0.1% poly(ethylene glycol) 8000. The solution is preincubated at the temperature of the assay for 15 min. The reaction is monitored for 5−15 min after adding 10 μL of the thrombin stock solution (9.0 nM) kept in ice. The temperature change (less than 0.15 °C) due to the addition of the thrombin soluton is ignored. Most of the inhibitors inhibit thrombin rapidly so that the steady state is achieved within a few minutes. The kinetic data (the steady-state velocity at various concentrations of the inhibitors) of the competitive inhibition are analyzed using the methods described by Segel (1975). Two inhibitors (P552 and P740 in Table 1) show a slow inhibition so that their steady-state velocities, v_s, are estimated from the following slow inhibition equation:

$$P = v_s t + (v_0 - v_s)(1 - e^{-kt})/k + d \qquad (2)$$

where P is the fluorescence intensity, v_0 is the initial velocity, d is the fluorescence intensity at $t = 0$, and k is a parameter relevant to the kinetic mechanism (Morrison & Stone, 1985). The equation below is then used to estimate the inhibition constant (K_i) at various temperatures:

$$v_s = V_{max}[S]/\{K_m(1 + [I]/K_i) + [S]\} + v_c \qquad (3)$$

where v_c is a parameter used to account for the deviation from linearity. A nonlinear regression program in Microsoft Excel is used to estimate the kinetic parameters (v_s, k, and d in eq 2 and K_m, V_{max}, and K_i in eq 3).

Molecular Modeling. The crystal structure of the thrombin−P500 complex (Féthière et al., 1996) is used as the starting point for molecular modeling. P500 is a bivalent thrombin inhibitor with the sequence dansyl-Arg-(D-Pip)-μAdod-Gly-Asp^{H55}-Phe-Glu-Glu-Ile-Pro^{H60}-Glu-Glu-Tyr-Leu-Gln^{H65}-OH and is homologous to P552, the reference inhibitor in the congeneric series studied in this paper (Table 1). The FRE inhibitor segments of P500 and P552 are identical. Since the series of inhibitors studied in this paper differ from each other only in the FRE segment, the active site and linker moiety are not included in our simulation. The bound state of the FRE segment is modeled using the sequence Ac-Asp^{H55}-Phe-Glu-Glu-Ile-Pro^{H60}-Glu-Glu-Tyr-Leu-Gln^{H65}-$NHCH_3$ docked in the FRE as in the thrombin−P500 crystal structure. Water molecules observed in the crystal structure are retained. The complex is then energy-minimized by allowing atoms of the FRE inhibitor segment as well as the thrombin residues and water molecules within 6 Å from any atom of the FRE inhibitor segment to move during minimization. The AMBER force-field (Weiner et al., 1986) as implemented in SYBYL 6.1 (Tripos Inc.) is used with a nonbonded cutoff of 8 Å, a dielectric constant of 80, and a gradient convergence tolerance of 0.005 kcal/(mol·Å).

This refined structure is the starting point for modeling the complexes of the Gly-substituted inhibitor analogs, in which Phe^{H56}, Ile^{H59}, Pro^{H60}, Tyr^{H63}, or Leu^{H64} are substituted in turn by Gly. The following two-step energy minimization is applied, first, after the Gly substitution, the energy of the complex at the FRE is minimized by allowing the inhibitor and water atoms to move while the thrombin structure is fixed. In the second step, the energy of the complex is minimized by allowing the atoms of the inhibitor, thrombin, and water molecules to be mobile. The energy minimization includes only the atoms of the inhibitor analog, thrombin, and water molecules, which are within 4 Å (5 Å when Leu^{H64} is substituted by Gly) from any atom of the Gly residue substituted.

Scheme 1

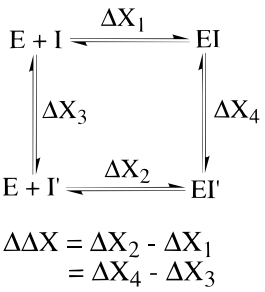

$$\Delta\Delta X = \Delta X_2 - \Delta X_1 = \Delta X_4 - \Delta X_3$$

Since P741(F56G) shows different thermodynamic profiles from other analogs of P552, a method which combines systematic conformational search and Monte Carlo energy-minimization (Wang et al., 1995) is applied for further study. The rotatable bonds of the backbone and the side chains are varied in 15° increments for (Phe^{H56} or Gly^{H56}) and Glu^{H57} and 30° increments for Asp^{H55} in the complex with thrombin in order to generate a database of sterically feasible conformations, where the water molecules are not included in the conformational search. The conformers in the database are sampled and energy-minimized. The free energy of the complex is given from the partition function of an ensemble consisting of the accepted low-energy conformers (Wang et al., 1995). A similar procedure is applied to the free state of the inhibitor, in which a truncated sequence, Ac-Asp^{H55}-(Phe^{H56} or Gly^{H56})-Glu^{H57}-$NHCH_3$, is used and all rotatable bonds are varied in 15° increments. The free energy of the free state is given from the partition function of an ensemble consisting of all possible energy levels of the truncated sequence. The free energy difference (ΔG_{bound} and ΔG_{free}) is the difference free energy between P552 and P741(F56G) in the bound and free states, respectively. The effect of Gly substitution of Phe^{H56} is then calculated as the relative free energy difference between ΔG_{bound} and ΔG_{free}.

Molecular Surface Calculation. The molecular surface is an envelope of a molecule from which the solvent is excluded (Richards, 1977). The molecular surface area is estimated using the GEPOL algorithm (Pascual-Ahuir et al., 1994) with the van der Waals radii used in the AMBER force-field (Weiner et al., 1986) and a solvent probe radius of 1.4 Å. The polar molecular surface is composed of oxygen, nitrogen, and polar hydrogens (e.g., NH and OH), and the nonpolar molecular surface is composed of all other atoms. Scheme 1 illustrates the change in the molecular surface area due to the Gly substitution. E is the enzyme (thrombin in this work), I is the reference inhibitor of P552, and I′ is the Gly substitution analog of P741(F56G), P740(I59G), P776(P60G), P751(Y63G), or P752(L64G) (see Table 1). By replacing the notation X by A, ΔA_1 and ΔA_2 are the changes of the surface area upon the binding of P552 and its analog to thrombin, respectively. ΔA_3 and ΔA_4 are the changes of the molecular surface area due to the loss of the side chain of Phe^{H56}, Ile^{H59}, Pro^{H60}, Tyr^{H63}, or Leu^{H64} in the free state and in the complex with thrombin, respectively. Consequently, $\Delta\Delta A$ ($=\Delta A_2 - \Delta A_1$) is the change of the molecular surface area upon the removal of the nonpolar side chain of

Phe^{H56}, Ile^{H59}, Pro^{H60}, Tyr^{H63}, or Leu^{H64}. The cycled process satisfies

$$\Delta A_1 + \Delta A_4 - \Delta A_2 - \Delta A_3 = 0 \quad (4)$$

Hence

$$\begin{aligned}\Delta\Delta A &= \Delta A_2 - \Delta A_1 \\ &= \Delta A_4 - \Delta A_3\end{aligned} \quad (5)$$

The free state of the inhibitor is modeled using the tripeptide Gly-Xaa-Gly, where Xaa stands for Phe, Ile, Pro, Tyr, Leu, or Gly. The backbone conformation of the tripeptide is set as $\psi = 140°$ and $\phi = -140°$. The side-chain conformations and their populations are determined based on the statistical survey of the side-chain conformations in 100 refined protein structures (Blaber et al., 1994). ΔA_3 is then calculated using the geometry of this tripeptide model. The assumption is that the surface area change in the free peptide is localized around the mutated residue. The surface area of free thrombin is, of course, unaffected by the mutation in the peptide. ΔA_4 is estimated based on the energy-minimized complex conformation. The surface area of the thrombin atoms, which are fixed in the energy minimization, is not affected by the mutation, and, hence, is not included in the calculation of ΔA_4.

RESULTS

Temperature Dependence of K_m and V_{max}. Human α-thrombin is stable in the temperature range (10−45 °C) used in this paper (Borgne & Graber, 1994). Figure 1A shows the temperature dependence of the enzymatic activity. As the substrate concentration is increased, the steady-state velocity becomes more sensitive to the temperature and shows the maximum at higher temperature. Figure 1B shows the temperature dependence of the enzymatic parameters, K_m and V_{max}, which are estimated at each temperature by nonlinear fitting of the equation:

$$v = V_{max}[S]/(K_m + [S]) \quad (6)$$

where v is the steady-state velocity and [S] is the substrate concentration. The temperature dependence of V_{max} is analyzed by nonlinear fitting of the equation:

$$\begin{aligned}V_{max} &= k_2[E]_T \\ &= A[E]_T e^{-E/RT}\end{aligned} \quad (7)$$

where k_2 is a kinetic constant of the substrate hydrolysis and $[E]_T$ is the total enzyme concentration (=30 pM), A is a constant related to the collision frequency, E is an activation energy derived from the Arrhenius equation, and R is a gas constant [=1.987 cal/(mol·K)]. The fitted values of the parameters E and A are 10.4 kcal/mol and 9.65×10^{11} s^{-1}, respectively. The dashed line in Figure 1B is the fitted curve of V_{max}. The temperature dependence of K_m is analyzed by using its relationship with the binding free energy as follows:

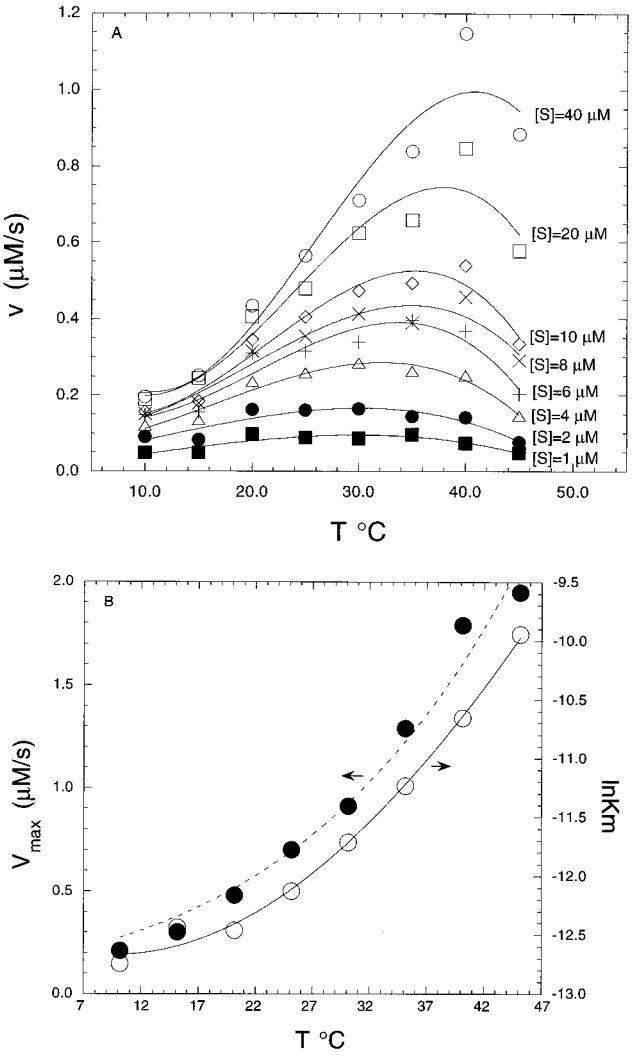

FIGURE 1: Temperature dependence of (A) enzymatic activity measured by the steady-state velocity (v) at the thrombin concentration of 30 pM, and of (B) Michaelis constant (K_m) and maximal velocity (V_{max}). The solid lines in panel A are the fitted curves using a polynomial equation. The dashed and solid lines in panel B are the fitted curves using eqs 7 and 8 in the text, respectively.

$$\begin{aligned}RT \ln K_m &\cong RT \ln K_d \\ &= \Delta G°(T) \\ &= \Delta H°(T) - T\Delta S°(T) \\ &= [\Delta H°(T°) - T\Delta S°(T°)] + \\ &\qquad \Delta C_p[(T - T°) - T \ln (T/T°)]\end{aligned} \quad (8)$$

Strictly speaking, $RT \ln K_d$ should be written as $RT \ln (K_d/a°)$, where $a°$ values are the concentrations of the various chemical species in their standard states. By taking 1.0 mol/L as a standard state, we are able to formally treat K_m and K_d as dimensionless quantities in eq 8. The fitted value of ΔC_p is -0.80 ± 0.09 kcal/(mol·K). The solid line in Figure 1B shows the fitting of the K_m data to eq 8. The values of $\Delta H°$ and $T\Delta S°$ are in good agreement with those published by Di Cera et al. (1991). The values for ΔC_p have not been previously reported. The nonlinear regression program in Microsoft Excel is used in the curve fittings of eqs 6−8.

The Inhibition Constant, K_i. Six inhibitors P552, P741-(F56G), P740(I59G), P776(P60G), P751(Y63G), and P752-(L64G), used in this study are listed in Table 1. P552 is a

Table 1: Sequences of the Synthetic Bivalent Thrombin Inhibitors

inhibitor	sequence
P552	Bbs-R-(D-Pip)-μAdod-γAbu-D^{H55}-F-E-E-I-P^{H60}-E-E-Y-L-Q^{H65}
P741(F56G)	Bbs-R-(D-Pip)-μAdod-γAbu-D^{H55}-**G**-E-E-I-P^{H60}-E-E-Y-L-Q^{H65}
P740(I59G)	Bbs-R-(D-Pip)-μAdod-γAbu-D^{H55}-F-E-E-**G**-P^{H60}-E-E-Y-L-Q^{H65}
P776(P60G)	Bbs-R-(D-Pip)-μAdod-γAbu-D^{H55}-F-E-E-I-**G**^{H60}-E-E-Y-L-Q^{H65}
P751(Y63G)	Bbs-R-(D-Pip)-μAdod-γAbu-D^{H55}-F-E-E-I-P^{H60}-E-E-**G**-**L**-Q^{H65}
P752(L64G)	Bbs-R-(D-Pip)-μAdod-γAbu-D^{H55}-F-E-E-I-PH60-E-E-Y-**G**-Q^{H65}
P1031(Y63F)	Bbs-R-(D-Pip)-μAdod-γAbu-D^{H55}-F-E-E-I-P^{H60}-E-E-**F**-L-Q^{H65}

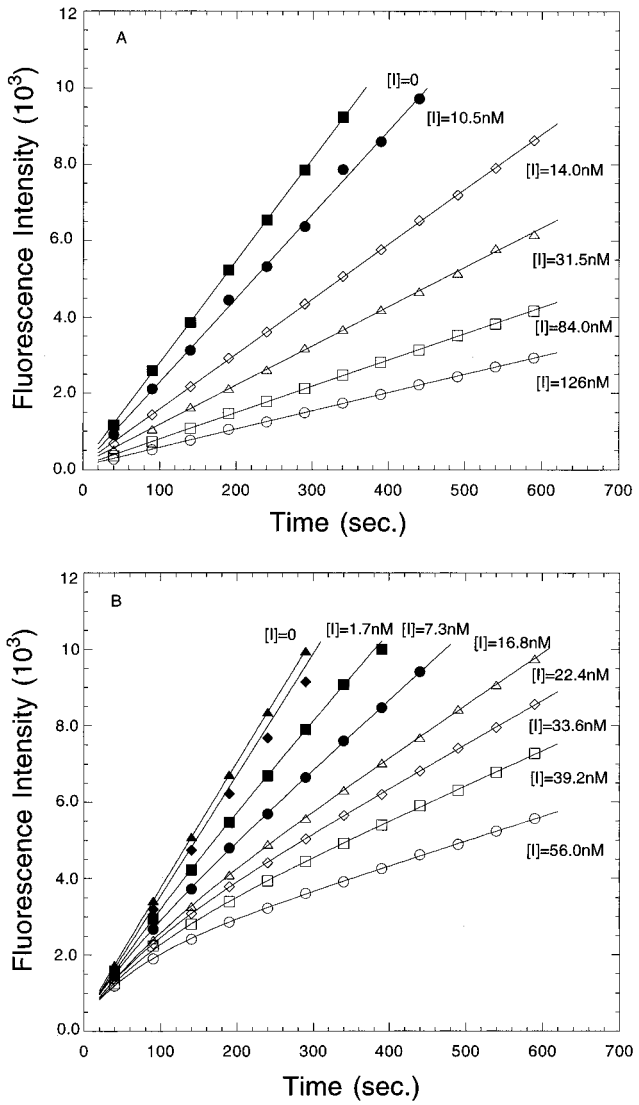

FIGURE 2: Hydrolysis of Tos-Gly-Pro-Arg-AMC (40 μM) by human α-thrombin (30 pM) in the presence of various concentrations of the inhibitors at 25 °C. The reaction is monitored by the fluorescence change with λ_{ex} of 383 nm and λ_{em} of 455 nm. Panel A shows a rapid inhibition of P741(F56G), and panel B shows a slow inhibition by P740(I59G).

reference inhibitor with the hirudin sequence at the FRE inhibitor segment. P741(F56G), P740(I59G), P776(P60G), P751(Y63G), and P752(L64G) are the analogs of P552 with the Gly substitution of Phe^{H56}, Ile^{H59}, Pro^{H60}, Tyr^{H63}, and Leu^{H64}, respectively. Figure 2A and Figure 2B show the rapid and slow inhibitions of thrombin activity by P741-(F56G) and P740(I59G), respectively. The steady-state velocity is used to determine the K_i values as described under Experimental Procedures. Table 2 shows the observed K_i values of these inhibitors at various temperatures. In general, the inhibitors are less efficient at higher temperature. The K_i values of P741(F56G) and P740(I59G) are 510- and 174-fold higher than that of P552 at 25 °C, respectively. Thus, the side chains of Phe^{H56} and Ile^{H59} in P552 play critical roles in the binding to the thrombin FRE. However, the Gly substitutions of Pro^{H60}, Tyr^{H63}, and Leu^{H64} do not affect the affinity of the inhibitor significantly, manifesting the weak contributions of the side chains of these residues in the binding.

Thermodynamic Profile. The K_i values are related to the thermodynamic properties through eq 1. The inhibition data in Table 2 fit well to eq 1, providing the thermodynamic parameters ($\Delta G°$, $\Delta H°$, and $T\Delta S°$, and ΔC_p) of the inhibition (Figure 3 shows an example of the fitting of P552). The nonlinear regression program in Microsoft Excel is used in the fitting, and the results are listed in Table 3. Only the fitted values of K_i, $\Delta G°$, $\Delta H°$, $T\Delta S°$, and ΔC_p are used in the following, unless specified as observed values. These values are based on the standard state of 1 mol/L and vary when other standard states, e.g., mole fraction, are used. However, their relative values ($\Delta\Delta G°$, $\Delta\Delta H°$, $T\Delta\Delta S°$, and $\Delta\Delta C_p$) have physical meaning by taking an appropriate inhibitor as a reference. In particular, by taking P552 as a reference inhibitor, the effect of the nonpolar side chains, which are removed in the analogs, is obtained from these relative values. The thermodynamic contributions from the unaffected parts in both the native and mutated inhibitors are canceled out in the relative values. The relative thermodynamic values are

$$\Delta\Delta X = \Delta X_2 - \Delta X_1 \qquad (9)$$

where ΔX_1 and ΔX_2 are the thermodynamic parameters ($\Delta G°$, $\Delta H°$, $T\Delta S°$, or ΔC_p) of P552 and its analog, respectively. $\Delta\Delta X$ is $\Delta\Delta G°$, $\Delta\Delta H°$, $T\Delta\Delta S°$, or $\Delta\Delta C_p$ and reflects the thermodynamic effect of the side chain of Phe^{H56}, Ile^{H59}, Pro^{H60}, Tyr^{H63}, or Leu^{H64} on the inhibitor binding to the thrombin FRE (Scheme 1). Table 4 lists the results. The removal of the Phe^{H56} side chain induces large changes in free energy (3.7 kcal/mol) and heat capacity [0.45 kcal/(mol·K)]. The small enthalpy change is rather unusual, considering the many interactions of the Phe^{H56} side chain with thrombin [a total of 10 hydrophobic contacts (Rydel et al., 1991)]. The negative value of the relative entropy is due to the entropy decrease of P741(F56G), whereas all other analogs increase the entropy (Table 3). This unusual behavior of the Phe^{H56} side chain is investigated further using molecular modeling as described later. The removal of the Tyr^{H63} side chain shows large increases in enthalpy and entropy but small increases in free energy and heat capacity. Contributions of other nonpolar side chains of Ile^{H59}, Pro^{H60}, and Leu^{H64} to the binding affinity are largely driven by enthalpy (Table 4). It should be mentioned that the Gly substitution of Ile^{H59} induces 3.1 kcal/mol of free energy increase at 25 °C, which is significantly smaller than the previously reported value of 5.0 kcal/mol at room temperature using another bivalent inhibitor of Ac-(D-Phe)-Pro-Arg-Pro-ζAph-γAbu-Asp^{H55}-Phe-Glu-Glu-Ile-Pro^{H60}-Glu-Glu-Tyr-Leu-Gln^{H65}-OH. The discrepancy may be related to the difference in the active-site inhibitor or linker segment and will be reported elsewhere (Cheng and Konishi, 1996, manuscript in preparation).

Molecular Modeling. The structures of five P552 analogs are modeled using the crystal structure of thrombin-P500 as described under Experimental Procedures. The Gly substitution of Ile^{H59}, Pro^{H60}, Tyr^{H63}, or Leu^{H64} induces minor

Table 2: Observed Inhibition Constant, K_i (nM), of the Bivalent Thrombin Inhibitors at Various Temperatures

T (°C)	P552	P741(F56G)	P740(I59G)	P776(P60G)	P751(Y63G)	P752(L64G)	P1031(Y63F)
10	0.00509	1.96	1.49	0.26	0.16	0.17	0.055
15	0.00575	2.55	1.27	0.17	0.23	0.21	0.067
20	0.00685	3.44	1.18	0.28	0.21	0.28	0.078
25	0.01144	5.83	1.99	0.54	0.15	0.36	0.13
30	0.01267	6.30	2.59	0.63	0.35	0.38	0.16
35	0.03237	12.27	4.22	0.61	0.30	0.50	0.20
40	0.05721	17.49	5.44	1.25	0.47	1.21	0.25
45	0.07436	22.98	5.93	2.36	0.84	1.66	0.58

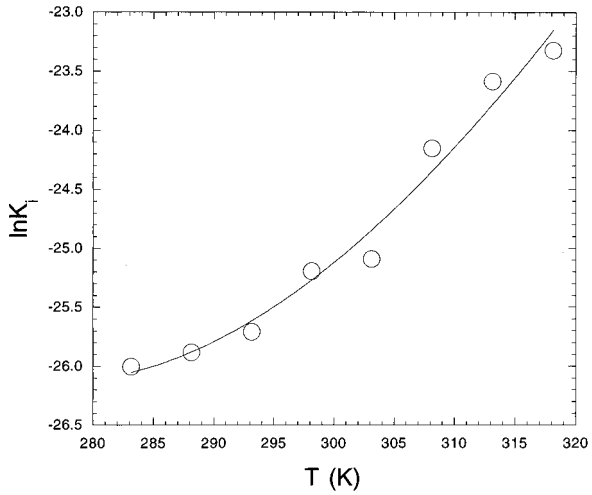

FIGURE 3: Temperature dependence of the inhibition constant (ln K_i) of the inhibitor P552. The solid line is the fitted curve using eq 1.

conformational adjustment of the neighboring side chains but does not affect the backbone conformation of the inhibitor or thrombin. The coordinates of the water molecules observed at the FRE in the crystal structure are unaffected. On the other hand, the Gly substitution of Phe^{H56} induces a large conformational change as the backbone of Asp^{H55}-Gly^{H56}-Glu^{H57} moves toward the binding pocket of the Phe^{H56} side chain (Figure 4). Also, three water molecules observed around this site in the crystal structure move closer to thrombin. As a result, Gly^{H56} interacts with Phe^{34}, Gln^{38}, Leu^{40}, Arg^{67}, Arg^{73}, and Thr^{74} of thrombin residues. Also, Arg^{73}, Thr^{74}, and Asp^{H55} form new hydrogen bonds with water molecules while maintaining the other hydrogen bonds of Asp^{H55} and Glu^{H57} with water observed in the thrombin−P500 complex. These interactions may largely compensate the enthalpy loss due to the removal of the Phe^{H56} side chain and may reduce the conformational flexibility (entropy) of the Asp^{H55}-Gly^{H56}-Glu^{H57} segment. In order to assess the validity of the large conformational change observed for Gly-substituted Phe^{H56}, the relative free energy of binding is calculated. The calculated free energy change ($\Delta\Delta G° = 3.9$ kcal/mol) is in good agreement with the experimental value of 3.7 kcal/mol at 25 °C. This suggests that the modeled conformational change is reasonable.

Molecular Surface. The molecular surface is classified into two groups, polar and nonpolar surfaces. As a first approximation, the polar and nonpolar atoms are assumed to have equal but opposite contribution to the hydrophobicity of the molecular surface (A_{net}), i.e.:

$$A_{net} = A_{npl} - A_{pol} \quad (10)$$

where "npl" and "pol" stand for nonpolar and polar, respectively. The changes in polar and nonpolar surface area are calculated using Scheme 1 and are listed in Table 5. In the free state, the Gly substitution of Phe^{H56}, Ile^{H59}, Pro^{H60}, Tyr^{H63}, and Leu^{H64} reduces the nonpolar surface area and, except for Tyr^{H63}, increases the polar surface area of the tripeptide (ΔA_3 in Table 5). In the bound state, the Gly substitution of Phe^{H56} and Ile^{H59} increases the nonpolar surface area and decreases the polar surface area, whereas the elimination of the nonpolar side chain from Pro^{H60}, Tyr^{H63}, or Leu^{H64} decreases the nonpolar surface area and increases the polar surface area (ΔA_4 in Table 5). As a result, $\Delta\Delta A_{npl}$ is increased by 129, 97, 35, 39, or 47 Å^2 in substituting Phe^{H56}, Ile^{H59}, Pro^{H60}, Tyr^{H63}, or Leu^{H64} with Gly, respectively, whereas $\Delta\Delta A_{pol}$ is decreased by 24, 18, or 16 Å^2 in substituting Phe^{H56}, Ile^{H59}, or Pro^{H60} with Gly, respectively, and is increased by 89 or 6 Å^2 in substituting Tyr^{H63} or Leu^{H64} with Gly, respectively. Consequently, there is a large increase in $\Delta\Delta A_{net}$ upon Gly substitution of Phe^{H56} and Ile^{H59} ($\Delta\Delta A_{net} = 153$ and 115 Å^2, respectively). The increase is less or even negative upon Gly substitution of Pro^{H60}, Tyr^{H63}, or Leu^{H64} ($\Delta\Delta A_{net} = 51$, −50, or 41 Å^2, respectively).

DISCUSSION

Thermodynamic Profile and Structure. Each hydrophobic side chain of the bivalent thrombin inhibitor, P552, at the FRE inhibitor segment contributes to the binding free energy in the range from 1.8 to 3.7 kcal/mol. The Gly substitution of Phe^{H56} is particularly interesting. The phenyl group of Phe^{H56} fills a hydrophobic pocket formed by the thrombin residues of Phe^{34}, Leu^{40}, Arg^{73}, and Thr^{74} (Zdanov et al., 1993). This pocket preexists in the PPACK−thrombin complex in the absence of FRE inhibitor (Bode et al., 1989). Upon binding the Phe^{H56} side chain, the loop 34−41 of thrombin moves toward Phe^{H56}, and Thr^{74} moves to close off the binding pocket. The observed movements are, however, small with a maximal displacement of about 2 Å in the side chain of Thr^{74} (Betz et al., 1991). Furthermore, it has been demonstrated that the replacement of Phe^{H56} by Leu, Ile, Val, Thr, Gln, His, or Glu significantly decreases the affinity of recombinant hirudin analogs or the FRE inhibitors whereas the substitution by Tyr, Trp, or Ala causes little change in the binding affinity (Krstenansky et al., 1990; Betz et al., 1991). Tyr and Trp are homologous to Phe; however, the small effect of Ala substitution is mysterious considering the elimination of the large phenyl group. Tsuda et al. (1995) suggested a large conformational change of the backbone of Ala^{H56} may compensate the loss of the phenyl group. The molecular modeling of P741(F56G) also shows that the backbone of Asp^{H55}-Gly^{H56}-Glu^{H57} moves close to the binding pocket and Gly^{H56} interacts with Phe^{34}, Gln^{38}, Leu^{40}, Arg^{40}, Arg^{67}, Arg^{73}, and Thr^{74} as shown in Figure 4.

Table 3: Binding Thermodynamics[a] of P552 and Its Analogues (25 °C)

inhibitor	K_i (nM)	$\Delta G°$ (kcal/mol)	$\Delta H°$ (kcal/mol)	$T\Delta S°$ (kcal/mol)	ΔC_p[b] [kcal/(mol·K)]
P552	0.011 ± 0.00	−14.97 ± 0.02	−13.66 ± 1.12	1.31 ± 1.13	−0.644 ± 0.211
P741(F56G)	5.20 ± 0.32	−11.30 ± 0.03	−12.74 ± 0.69	−1.44 ± 0.70	−0.193 ± 0.131
P740(I59G)	1.94 ± 0.03	−11.88 ± 0.01	−8.08 ± 1.23	3.80 ± 1.24	−0.439 ± 0.232
P776(P60G)	0.39 ± 0.08	−12.84 ± 0.10	−10.73 ± 1.62	2.11 ± 1.64	−0.573 ± 0.305
P751(Y63G)	0.21 ± 0.03	−13.19 ± 0.11	−6.07 ± 1.57	7.12 ± 1.58	−0.623 ± 0.294
P752(L64G)	0.32 ± 0.02	−12.95 ± 0.04	−10.22 ± 1.04	2.73 ± 1.05	−0.532 ± 0.197
P1031(Y63F)	0.093 ± 0.01	−13.68 ± 0.10	−9.88 ± 0.42	3.80 ± 1.27	−0.626 ± 0.081

[a] The fitted values are listed with the standard deviation of the fitting for each parameter. [b] ΔC_p is assumed to be temperature-independent.

Table 4: Effect of Nonpolar Side Chains of the FRE Inhibitor Segment, Hirudin$^{55-65}$, on the Binding Thermodynamics at 25 °C

substitution of inhibitors	K_i'/K_i[a]	$\Delta\Delta G°$ (kcal/mol)	$\Delta\Delta H°$ (kcal/mol)	$T\Delta\Delta S°$ (kcal/mol)	$\Delta\Delta C_p$ [kcal/(mol·K)]
Phe56Gly	473	3.7	0.92	−2.8	0.45
Ile59Gly	176	3.1	5.6	2.5	0.21
Pro60Gly	35	2.1	2.9	0.80	0.071
Tyr63Gly	19	1.78	7.6	5.8	0.021
Leu64Gly	29	2.0	3.4	1.4	0.112
Phe63Gly	2.3[b]	0.49	3.8	3.3	0.003

[a] K_i and K_i' are the fitted inhibition constants of P552 and its analogs [P741(F56G), P740(I59G), P776(P60G), P751(Y63G), or P752(L64G)], respectively, in Table 3. [b] K_i and K_i' are, as an exception, the fitted inhibition constants of P1031(Y63F) and P751(Y63G).

These interactions of Gly^{H56} and the newly formed hydrogen bonds with water molecules may largely compensate the Phe^{H56} side chain interactions, resulting in a small enthalpy change ($\Delta\Delta H° = 0.92$ kcal/mol in Table 4) upon Gly substitution of Phe^{H56}. Also, the negative entropy change ($T\Delta\Delta S° = -2.8$ kcal/mol in Table 4) may be largely attributed to the rigid conformation of the Asp^{H55}-Gly^{H56}-Glu^{H57} backbone in the complex. A similar thermodynamic profile (a small $\Delta\Delta H°$ and a negative $T\Delta\Delta S°$) and conformational change is observed in a double-substitution of Tyr^{H63}-Leu^{H64} by Gly-Gly (data not shown). In contrast, the Gly substitution of Ile^{H59}, Pro^{H60}, Tyr^{H63}, or Leu^{H64} shows a large enthalpy increase and entropy increase, and no significant backbone movement in the modeled complexes. Thus, a small enthalpy change with a significant entropy loss in eliminating side chain(s) may imply a conformational change being induced.

Correlations among the Thermodynamic Parameters. Hopfner et al. (1993) reported the thermodynamic profile of the binding of hirudin, fibrinogen, and the synthetic bivalent thrombin inhibitors to thrombin. A Krug−Hunter−Grieger plot (Krug et al., 1976a,b) of these substrate and inhibitors shows a quadratic relationship between ΔH and ΔG. The thermodynamic profile of some inhibitors listed in Table 1, however, does not fit to the quadratic expression, and the ΔG shows no correlation with ΔH or ΔS at either 37 °C (data not shown) or 25 °C (Table 3). On the other hand, a plot of $\Delta\Delta H°$ vs $\Delta\Delta S°$ in Figure 5 shows a very good compensation effect between the enthalpy and entropy changes. Our data are supplemented with those of Hopfner et al. (1993).[3] The data of $\Delta\Delta H°$ and $\Delta\Delta S°$ in Figure 5 reflect minor modifications of the bivalent inhibitors which eliminate a nonpolar side chain at the FRE inhibitor segment or introduce an amide bond at the linker. The linear least-squares fit the data in Figure 5 is given by

$$\Delta\Delta H° = 312\Delta\Delta S° + 1.48 \qquad r^2 = 0.91 \qquad (11)$$

The slope in eq 11 is known as the compensation temperature and is generally in a relatively narrow range from 250 to 315 K (Lumry & Rajender, 1970). Our value of 312 lies within this range. A strong enthalpy−entropy correlation is also observed in $\Delta H°$ and $\Delta S°$ values in Table 3, including the data of the synthetic bivalent inhibitors reported by Hopfner et al. (1993). Enthalpy−entropy correlation has been observed in other studies. The binding of ligands to receptors shows the strong enthalpy−entropy correlation in a wide range of $\Delta H°$ (−25 to 35 kcal/mol) and $\Delta S°$ [−0.05 to 0.15 kcal/(mol·K)] (Gilli et al., 1994). Protein stability studies show that approximately 90% of the interaction energy (ΔH = 50−200 kcal/mol) is compensated by the entropy loss, resulting in 5−15 kcal/mol of free energy stabilization (Privalov, 1979; Shortle et al., 1988).

Molecular Surface and Free Energy. Horton and Lewis (1992) found a very good correlation between dissociation free energy and interface area in 15 protein−protein complexes. This correlation may be too simplified and cannot be valid in general, because specific interactions such as hydrogen bonding and ion pairs are sensitive to the detailed atomic structure (Janin, 1995). However, the less specific interactions such as hydrophobic interactions may show similar correlation, although the molecular surface must be carefully estimated. In this paper, we take into account the molecular surfaces of not only the complex but also the dissociated molecules. Then, the values of $\Delta\Delta G°$ in Table 4 show a very good correlation with $\Delta\Delta A_{net}$ in Table 5. An exception is the Gly substitution of Tyr^{H63}. The reason that Y63G is an outlier may be that the tyrosyl side chain contains a hydroxyl group that could be involved with a specific hydrogen bonding interaction (e.g., with Tyr^{76}). The surface area calculation would not reflect the loss of such a specific interaction. In order to examine the contribution of a benzyl side chain of the 63rd residue, the thermodynamic properties of Phe^{H63} are compared to those of Gly^{H63}. The inhibition constant and the thermodynamic values of P1031(Y63F) are listed in Tables 2−4. Unlike the corresponding mutation in recombinant hirudin where the K_i values increase only 13%, the substitution of Tyr^{H63} in P552 by Phe reduces the affinity by 9-fold. Thus, the hydroxyl group contributes more than the benzyl group in the binding affinity of the synthetic

[3] The values in Figure 5 refer to the values at 25 °C. Although the data of Hopfner et al. (1993) were measured at 37 °C, $\Delta\Delta H$ and $\Delta\Delta S$ were analyzed as temperature-independent. A bivalent inhibitor (P201), Ac-(D-Phe)-Pro-Arg-μAdod-hirudin$^{55-65}$, is used as a reference inhibitor to estimate $\Delta\Delta H$ and $\Delta\Delta S$, because it has no amide bond in the linker.

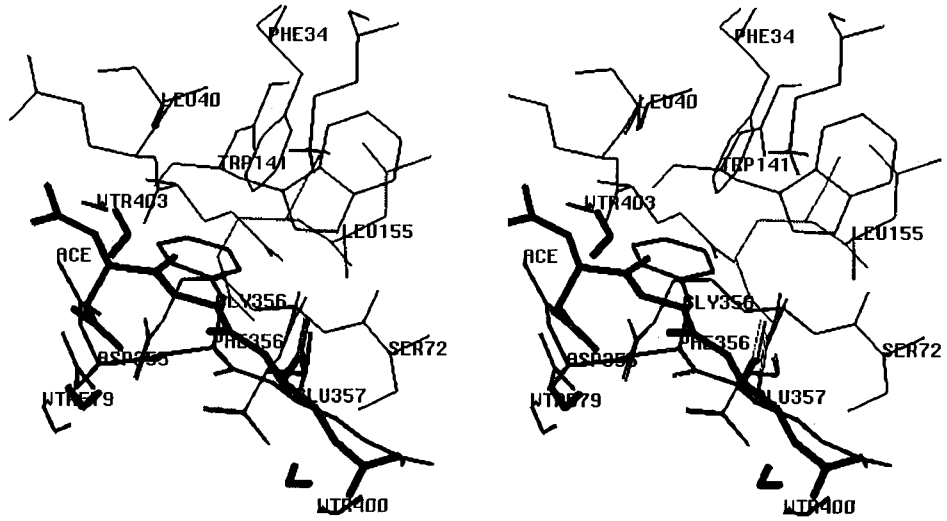

FIGURE 4: Stereoview of thrombin−P552 and thrombin−P741(F56G) complexes at around the 56th residue of the inhibitors. Since thrombin structures are almost superimposable in both complexes, only the low-energy structure of thrombin in the complex with P552 is shown in the figure (thin connections). The structures of P552 and P741(F56G) are shown with medium and thick connections, respectively.

Table 5: Polar and Nonpolar Molecule Surfaces of Thrombin and Inhibitors in the Complex and in the Free State

	ΔA_3 (Å^2)		ΔA_4 (Å^2)		$\Delta\Delta A$ (Å^2)[a]		
substitution of inhibitors	polar	nonpolar	polar	nonpolar	polar	nonpolar	$\Delta\Delta A_{net}$ (Å^2)[b]
Phe56Gly	8	−106	−16	23	−24	129	153
Ile59Gly	12	−84	−6	13	−18	97	115
Pro60Gly	17	−62	1	−27	−16	35	51
Tyr63Gly	−14	−89	75	−50	89	39	−50
Leu64Gly	10	−84	16	−37	6	47	41
Phe63Gly	8	−106	100	−68	92	38	−54

[a] $\Delta\Delta A = \Delta A_4 - \Delta A_3$. [b] $\Delta\Delta A_{net} = \Delta\Delta A_{npl} - \Delta\Delta A_{pol}$.

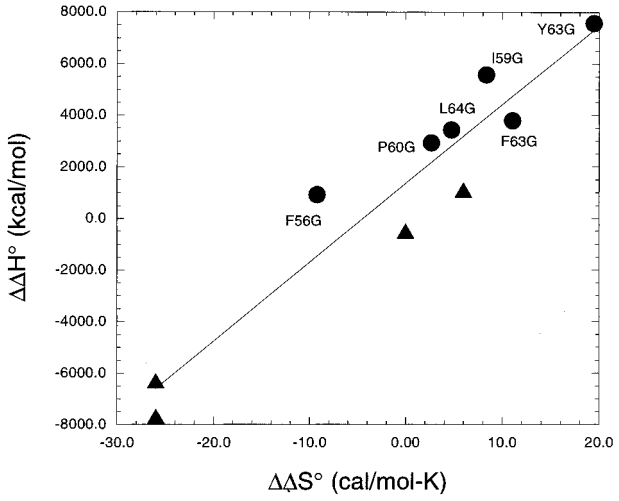

FIGURE 5: Correlation of $\Delta\Delta H°$ with $\Delta\Delta S°$ by taking P552 as a reference compound at 25 °C. The inhibitor residue substituted by Gly is noted beside each filled circle. The figure also includes the data (filled triangle) of Hopfner et al. (1993) by taking P201 as a reference compound because of its simplest linker structure, μAdod.

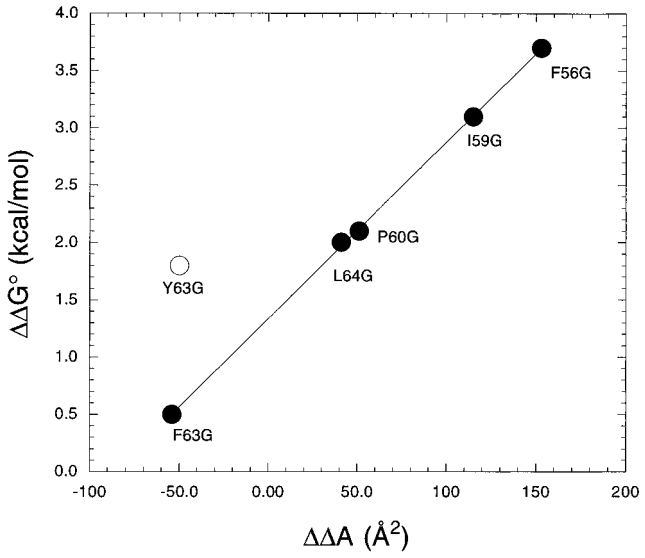

FIGURE 6: Correlation of molecular surface change ($\Delta\Delta A_{net} = \Delta\Delta A_{npl} - \Delta\Delta A_{pol}$) with the relative binding free energy change. The solid linear line is the linear least-squares fitting with a correlation of $\Delta\Delta G° = 0.0154\Delta\Delta A_{net} + 1.34$ ($r^2 = 1.00$). The data of the Gly substitution of Tyr^{H63} are excluded from the fitting as described in the text.

inhibitor. The least-squares fitting of $\Delta\Delta G°$ vs $\Delta\Delta A_{net}$ (Figure 6) yields

$$\Delta\Delta G° = 0.0154\Delta\Delta A_{net} + 1.34 \qquad r^2 = 1.00 \quad (12)$$

where the data of Tyr^{H63} are replaced by those of Phe^{H63}. The strong correlation between the free energy and the surface area change is further supported by four other analogs of the synthetic bivalent inhibitors (unpublished results). Consequently, the complex stability due to the hydrophobic interactions is well reflected by the molecular surface change upon complex formation. However, it should be pointed out that the linear correlation of eq 12 may not be applicable to other types of interactions as already implied by the Gly substitution of Tyr^{H63} in Figure 6. Nevertheless, the good correlation obtained from surface area calculations based on

modeled structures suggests the feasibility of predicting relative binding affinities for a congeneric series of inhibitors.

CONCLUSION

Thermodynamic analysis of the nonpolar interactions between the FRE of thrombin and the hirudin-based inhibitors provides detailed information of the molecular association. The nonpolar interactions of Ile^{H50}, Pro^{H60}, Tyr^{H63}, and Leu^{H64} side chains are enthalpy-driven such that van der Waals interactions play the major role in the molecular association. The Gly substitution of Phe^{H56} is exceptionally entropy-driven, and molecular modeling predicts a large conformational change of P741(F56G) to compensate the loss of the benzyl group. Nevertheless, a strong compensation between enthalpy and entropy is observed in all Gly substitution analogs. A careful investigation of the thermodynamic parameters and the structure of the Gly substitution analogs shows, for the first time, a very good correlation between the affinity of the molecular association and the hydrophobicity of the molecular surface.

ACKNOWLEDGMENT

We thank Jean Lefebvre and Bernard F. Gibbs for their technical assistance in the peptide synthesis and amino acid analysis, and Hervé Hogues for his programming assistance in the molecular modeling and molecular surface calculation.

REFERENCES

Baldwin, R. L. (1986) *Proc. Natl. Acad. Sci. U.S.A. 83*, 8069−8072.
Betz, A., Hofsteenge, J., & Stone, S. R. (1991) *Biochemistry 30*, 9848−9853.
Blaber, M., Zhang, X., Lindstrom, J. D., Pepiot, S. D., Baase, W. A., & Matthews, B. W. (1994) *J. Mol. Biol. 235*, 600−624.
Bode, W., Mayer, I., Baumann, U., Huber, R., Stone, S. R., & Hofsteenger, J. (1989) *EMBO J. 8*, 3467−3475.
Borgne, S. L., & Graber, M. (1994) *Appl. Biochem. Biotechnol. 48*, 125−135.
Chaturvedi, D. N., Knittel, J. J., Hruby, V. J., Castrucci, A. M., & Hadley, M. E. (1984) *J. Med. Chem. 27*, 1406−1410.
Clore, G. M., Sukumaran, D. K., Nilges, M., Zarbock, J., & Groneborn, A. M. (1987) *EMBO J. 6*, 529−537.
Di Cera, E., De Cristofaro, R., Albright, D. J., & Fenton, J. W., II (1991) *Biochemistry 30*, 7913−7924.
Féthière, J., Tsuda, Y., Coulombe, R., Konishi, Y., & Cygler, M. (1996) *Protein Sci. 5*, 1174−1183.
Folkers, P. J. M., Clore, G. M., Driscoll, P. C., Dodt, J., Köhler, S., & Gronenborn, A. M. (1989) *Biochemistry 28*, 2601−2617.
Gilli, P., Ferretti, V., Gilli, G., & Borea, P. A. (1994) *J. Phys. Chem. 98*, 1515−1518.
Gould, R. J., & Shafer, J. A. (1993) *Perspect. Drug Discovery Des. 1*, 419−422.
Grütter, M. G., Priestle, J. P., Rahuel, J., Grossenbacher, H., Bode, W., Hofsteenge, J., & Stone, S. R. (1990) *EMBO J. 9*, 2361−2365.
Haruyama, H., & Wüthrich, K. (1989) *Biochemistry 28*, 4301−4312.
Hopfner, K.-P., & Di Cera, E. (1992) *Biochemistry 31*, 11567−11571.
Hopfner, K.-P., Ayala, Y., Szewczuk, Z., Konishi, Y., & Di Cera, E. (1993) *Biochemistry 32*, 2947−2953.
Horton, N., & Lewis, M. (1992) *Protein Sci. 1*, 169−181.
Janin, J. (1995) *Biochimie 77*, 497−505.
Karshikov, A., Bode, W., Tulinsky, A., & Stones, S. R. (1992) *Protein Sci. 1*, 727−735.
Krstenansky, J. L., Broersma, R. J., Owen, T. J., Payne, M. H., Yates, M. T., & Mao, S. J. T. (1990) *Thromb. Haemostasis 63*, 208−214.
Krug, R. R., Hunter, W. G., & Grieger, R. A. (1976a) *J. Phys. Chem. 80*, 2335−2341.
Krug, R. R., Hunter, W. G., & Grieger, R. A. (1976b) *J. Phys. Chem. 80*, 2341−2351.
Lefkovits, J., & Topol, E. J. (1994) *Circulation 90*, 1522−1536.
Lumry, R., & Rajender, S. (1970) *Biopolymer 9*, 1125−1227.
Makhatadze, G. I., & Privalov, P. L. (1993) *J. Mol. Biol. 232*, 639−659.
Markwardt, F. (1989) *Semin. Thromb. Hemostasis 15*, 269−282.
Morrison, J. F., & Stone, S. R. (1985) *Comments Mol. Cell Biophys. 2*, 347−368.
Murphy, K. P., & Freire, E. (1992) *Adv. Protein Chem. 43*, 313−361.
Murphy, K. P., Privalov, P. L., & Gill, S. J. (1990) *Science 247*, 559−561.
Pascual-Ahuir, J. L., Silla, E., & Tuñón, I. (1994) *J. Comput. Chem. 15*, 1127−1138.
Privalov, P. L. (1979) *Adv. Protein Chem. 33*, 167−241.
Richards, F. M. (1977) *Annu. Rev. Biophys. Bioeng. 6*, 151−176.
Rydel, T. J., Ravichandran, K. G., Tulinksy, A., Bode, W., Huber, R., Roitsch, C., & Fenton, J. W., II (1990) *Science 249*, 277−280.
Rydel, T. J., Tulinsky, A., Bode, W., & Huber, R. (1991) *J. Mol. Biol. 221*, 583−601.
Segel, I. H. (1975) *Enzyme Kinetics: Behavior and Analysis of Rapid Equilibrium and Steady-State Enzyme Systems*, pp 100−160, John Wiley & Sons, New York.
Shortle, D., Meeker, A. K., & Freire, E. (1988) *Biochemistry 27*, 4761−4768.
Spolar, R. S., Ha, J., & Record, M. T., Jr. (1989) *Proc. Natl. Acad. Sci. U.S.A. 86*, 8382−8385.
Spolar, R. S., Livingstone, J. R., & Record, M. T., Jr. (1992) *Biochemistry 31*, 3947−3955.
Stone, S. R., & Hofsteenge, J. (1986) *Biochemistry 25*, 4622−4628.
Stone, S. R., Dennis, S., & Hofsteenge, J. (1989) *Biochemistry 28*, 6857−6863.
Szewczuk, Z., Gibbs, B. F., Yue, S.-Y., Purisima, E. O., & Konishi, Y. (1992) *Biochemistry 31*, 9132−9140.
Tsuda, Y., Szewczuk, Z., Wang, J., Yue, S.-Y., Purisima, E. O., & Konishi, Y. (1995) *Biochemistry 34*, 8708−8714.
Wang, J., Szewczuk, Z., Yue, S.-Y., Tsuda, Y., Konishi, Y., & Purisima, E. O. (1995) *J. Mol. Biol. 253*, 473−492.
Weiner, S. J., Kollman, P. A., Nguyen, D. T., & Case, D. A. (1986) *J. Comput. Chem. 7*, 230−252.
Yue, S.-Y., DiMaio, J., Szewczuk, Z., Purisima, E. O., Ni, F., & Konishi, Y. (1992) *Protein Eng. 5*, 77−85.
Zdanov, A., Wu, S., DiMaio, J., Konishi, Y., Li, Y., Wu, X., Edwards, B. F. P., Martin, P. D., & Cygler, M. (1993) *Proteins: Struct., Funct., Genet. 17*, 252−265.

BI961039C